



Porous nanostructured poly-L-lactide scaffolds prepared by phase inversion using supercritical CO₂ as a nonsolvent in the presence of ammonium bicarbonate particles

Aihua Deng^a, Aizheng Chen^{a,b}, Shibin Wang^{a,b,*}, Yi Li^{c,**}, Yuangang Liu^{a,b}, Xiaoxia Cheng^a, Zheng Zhao^c, Dongliang Lin^a

^a College of Chemical Engineering, Huaqiao University, Xiamen 361021, China

^b Institute of Pharmaceutical Engineering, Institute of Biomaterials and Tissue Engineering, Huaqiao University, Xiamen 361021, China

^c Institute of Textiles and Clothing, The Hong Kong Polytechnic University, Hung Hom, Kowloon 999077, Hong Kong, China

ARTICLE INFO

Article history:

Received 23 November 2012

Received in revised form 18 February 2013

Accepted 22 February 2013

Keywords:

Ammonium bicarbonate

Phase inversion

Scaffolds

Supercritical fluids

Tissue engineering

ABSTRACT

Supercritical fluid technology has been utilized in the development of tissue engineering scaffolds. However, it results in some problems, such as the poorly interconnected pores and the inability to load growth factor due to the salt leaching process for removal of the solid porogen. In this study, ammonium bicarbonate (AB) particles were used as a porogen and mixed uniformly with poly-L-lactide (PLLA) solution. Supercritical CO₂ was used to immerse and flush through the resulting compound to allow the occurrence of phase inversion, subsequently generating a nanofibrous network. As the decomposition temperature of AB crystals is 36 °C, the temperature of the CO₂ was increased to 40 °C to decompose the porogen, and the decomposition products were removed by washing with CO₂. The resulting PLLA scaffolds possessed both large pores and micro pores with a controllable pore size, a high porosity (>95%), an interconnected structure, a nanofibrous network, good mechanical properties (compressive strength up to 100 kPa), and a very low organic solvent residue (12 ppm). The results of Fourier transform infrared spectroscopy (FTIR) and X-ray diffraction (XRD) measurements indicated that the molecular structure and physical state of PLLA were not changed after supercritical processing. The results reveal that the application of AB particles as a porogen in the supercritical phase inversion process is feasible to produce tissue engineering scaffolds with a high-performance.

© 2013 Elsevier B.V. All rights reserved.

1. Introduction

PLLA is a biodegradable aliphatic polyester derived from renewable resources; it has been extensively studied and used in the area of industrial packaging and biomedical applications such as surgical implants, controlled drug delivery devices, and scaffolds for tissue engineering [1–3]. PLLA has been processed in different forms, such as particles, fibers and membranes, to be used in tissue engineering applications [4–6]. In these applications, PLLA scaffolds have been described as delivery systems capable of carrying active agents or bio-molecules and growth factors [7,8].

As an important part of tissue engineering, three-dimensional (3D) scaffolds play a pivotal role in cell seeding, cell prolifera-

tion, and new tissue formation [9]. One of the most important stages of building scaffolds is the design and processing of a porous 3D structure with high porosity, high interconnectivity, and uniform distribution of the pores. A variety of processing techniques have been developed and include particle leaching, gas foaming processes, thermally induced phase separation, and nonsolvent-induced phase inversion [10–13]. The main disadvantages of these methods are the use of organic solvents and the high temperatures required. Since the presence of residual organic solvents is being rigorously controlled by the international safety regulations, it is necessary to warrant the complete removal of these substances. Therefore, supercritical fluid technology appears to be an interesting alternative to the traditional processing method [14,15].

Nonsolvent-induced phase inversion technology has been widely used for fabricating porous polymer scaffolds [16,17]. During the process of fabricating porous polymer scaffolds, a nonsolvent was added into a homogeneous polymer solution, which leads to the separation of the polymer solution into a polymer-rich phase and a polymer-lean phase. The polymer-rich phase develops a continuous matrix while the polymer-lean phase mainly

* Corresponding author at: College of Chemical Engineering, Huaqiao University, Xiamen 361021, China. Tel.: +86 592 6162288; fax: +86 592 6162288.

** Corresponding author. Tel.: +86 852 2766479; fax: +86 852 2766479.

E-mail addresses: sbwang@hqu.edu.cn, azchen@hqu.edu.cn (S. Wang), ctliyi@polyu.edu.hk (Y. Li).

consisting of the solvent leads to generate porous tunnels within the matrix, thus forming a continuous, interconnected porous structure [18]. The supercritical CO₂ can be used as a nonsolvent instead of organic solvents, and this adds several advantages to the process. One of the most important advantages of using supercritical CO₂ is the fact that the final structure of the product can be tailored by simply tuning the operating parameters of pressure and temperature [19]. Moreover, when CO₂ is used as a nonsolvent, the collapse of the structure will not occur during the drying process due to the absence of a liquid–vapor interface, and the porous structure is free of any residual solvents [20].

Recently, a process in which supercritical CO₂ replaces the liquid nonsolvent for phase separation has been proposed [21], but the porous scaffolds prepared by the gas foaming techniques using supercritical CO₂ have a relatively closed pore network [22,23]. To overcome this issue, an additional porogen (sodium chloride particles) was incorporated into the compression molding of polymer before gas foaming. After gas foaming, the porogen was leached out by incubation in water for 48 h, thus creating a scaffold with an interconnected pore network [24]. However, the leaching of the porogen is a major disadvantage of this process, since it results in loss of the majority of any incorporated growth factors [25]. If the porogen in the scaffold was replaced by AB particles, the problem of the growth factor loss would be resolved, since the AB particles would break down at temperatures above 36 °C.

In this work, we attempted to produce a porous nanostructured PLLA scaffold with interconnected pores by phase inversion, using supercritical CO₂ as a nonsolvent in the presence of AB particles. Briefly, the AB particles were added to the PLLA solution and mixed vigorously, and then the polymer/salt/solvent paste was cast into the steel mold. The resulting compound was immersed in supercritical CO₂ to allow the occurrence of phase separation. Afterwards, the system was flushed with supercritical CO₂ for another 2 h to generate a nanofibrous network. As the decomposition temperature of AB crystals is 36 °C, the temperature of the CO₂ was increased to about 40 °C to decompose the porogen, and the decomposition products were removed by washing with CO₂.

2. Materials and methods

2.1. Materials

PLLA with an inherent viscosity of 3.5 dl/g (0.1% (wt/v) in chloroform, 25 °C) was purchased from the Jinan Daigang Biological Co., Ltd. (Jinan, China). AB and dichloromethane (99.8% purity) were bought from the Sinopharm Chemical Reagent Co., Ltd. (Shanghai, China), and CO₂ of 99.9% purity was purchased from the Rihong Air Products Co., Ltd. (Xiamen, China). All materials were used as received.

2.2. Methods

2.2.1. Scaffold preparation

PLLA was firstly dissolved in different solvents, namely dichloromethane, 1,4-dioxane, and dichloromethane/1,4-dioxane (1:1, v: v); the solution was stirred until it became homogeneous. Then, AB particles (size range 300–600 μm) were added into the solution and mixed vigorously. The AB/PLLA (w:w) ratios ranged from 10 to 40 and the concentration of PLLA was set as 10% (wt/v). The polymer/salt/solvent paste was cast into the steel mold, and then the resulting compound with a diameter of 2.0 cm and height of 5.0 mm was placed in the high-pressure vessel. Supercritical CO₂ was pumped into the high-pressure vessel to the desired pressure (15 MPa) and temperature (35 °C). After treatment for 2 h, the vessel was flushed with fresh CO₂ with a constant flow rate

(approximately 5 g/min) for 2 h to remove the organic solvent. During this process, the pressure and temperature were kept constant. Then, the system was rapidly depressurized to atmospheric pressure within 2 min. The temperature in the high-pressure vessel was increased to 40 °C, and the scaffold was flushed at a constant flow rate (approximately 5 g/min) until the AB particles were completely decomposed.

2.2.2. Scanning electron microscopy (SEM)

PLLA scaffolds were fractured in liquid nitrogen. Samples were sputter coated with gold for 180 S (Ion Sputter E-1010, Hitch, Japan). The overall scaffold structure was analyzed using a scanning electron microscope (SEM S-4800, Hitch, Japan).

2.2.3. Scaffold porosity

The “void space” of the scaffold was represented by the porosity (ε); the scaffold porosity was calculated by the equation below.

$$\varepsilon = 1 - \frac{\rho_s}{\rho_p}$$

where ρ_s is the density of the scaffold (scaffold weight/scaffold volume, g/cm³) and ρ_p is the density of as received PLLA (1.24 g/cm³).

2.2.4. Mechanical tests

The compressive mechanical properties of the scaffolds were measured on a UTM 6102 (Suns Co., Ltd., Shenzhen, China) equipped with a 0.1 kN load cell at room temperature. Cylindrical samples with a diameter of 2.0 cm and height of 5.0 mm were used. The cross-head speed was set at 1.0 mm/min. The compressive strength at 25% strain was determined by the ISO 604:2002.

2.2.5. Solvent residue analysis

Dichloromethane and 1,4-dioxane residue was measured using a headspace sampler (G1888, Agilent Technologies, USA) coupled to a gas chromatograph (GC) interfaced with a flame ionization detector (6890N, Agilent Technologies, USA).

2.2.6. FTIR analysis

Samples of approximately 1 mg were pressed into a pellet with 200 mg of potassium bromide, and FTIR spectra were collected in continuous scan mode (wavelength range: 4000–400 cm⁻¹) and at a resolution of 10 cm⁻¹ on a Nicolet iS10 system (Thermo, USA).

2.2.7. XRD analysis

XRD analysis was carried out using a PANalytical X'Pert PRO. The measurement was performed in the range of 10–35° with a step size of 0.013° in 2θ using Cu K α radiation as the source.

2.2.8. Differential scanning calorimetry (DSC) analysis

The melting behavior of PLLA scaffolds was investigated by employing a Netzsch DSC 200F3 differential scanning calorimeter. The calibration was performed with indium and all tests were carried out in ultra-pure nitrogen as the purge gas. Samples were heated from 30 °C to 200 °C at a rate of 10 °C/min.

2.2.9. Statistical analysis

All data presented are expressed as mean \pm standard deviations (SD). ANOVA single factor analysis were conducted, with the level of statistical significance set at $P < 0.05$. Every experiment was carried out in triplicate ($n = 3$).

3. Results and discussion

3.1. Surface morphology

In this work, the possibility of preparing PLLA scaffolds for tissue engineering using a supercritical assisted phase inversion technique in the presence of AB particles were evaluated.

Using conventional methods to produce scaffolds, in order to improve the porosity and interconnectivity of the scaffold, researchers have modified the process and proposed a hybridization of the supercritical fluids process with particulate leaching [26,27]. They introduced an insoluble porogen into the polymeric solution, such as D-fructose or sodium chloride particles. In order to eliminate the porogen in this process, the whole scaffold must be immersed in water or organic solvent for a long time to dissolve the particles [28]; this may lead to the loss of growth factor in the scaffold [25]. Sometimes, the samples were immersed into an excess amount of hot water (90 °C) to decompose the porogen, which may lead to the denaturation of the growth factor in the scaffold [29].

In this study, we selected AB particles of controlled size as the porogen, since it is insoluble in supercritical CO₂ and will break down at temperatures above 36 °C [29]. During the supercritical CO₂ processing, the temperature was kept at 35 °C. After the formation of a nanofibrous network, the AB particles were removed by increasing the temperature to 40 °C, to obtain an interconnected nanofibrous structure. This avoids the leaching process, which will denature the bioactive substances loaded in the scaffolds. According to the SEM images of PLLA scaffolds prepared under different pressures (as shown in Fig. S1 of Supplementary Material), it is found that the influence of pressures on the surface morphology of scaffolds was not significant; hence the operating pressure was set as 15 MPa in this study.

Supplementary material related to this article found, in the online version, at <http://dx.doi.org/10.1016/j.supflu.2013.02.020>.

Fig. 1 represents the optical image of the PLLA scaffold, which indicates that the shape and 3D structure of the tissue to be substituted could be reproduced accurately by the supercritical-CO₂-assisted phase inversion process. In the phase inversion process, the properties of the final porous structure are mainly controlled by the precipitation temperature, the pressure of the vessel, the flow rate of CO₂, and the concentration of the casting solution [23]. The role of the organic solvent in the morphology of the matrixes obtained was discussed only a few times in the supercritical-CO₂-assisted phase inversion technique. By the phase inversion with supercritical CO₂ as a nonsolvent, chitosan may form a dense membrane from formic acid, a macro-void structure with a dense layer on top from HFIP solution and a homogeneous scaffold from acetic acid solution [19]. Matsuyama [20] investigated the influence of four kinds of organic solvents on the porous cellulose acetate membranes; they found that as the mutual affinity decreased between solvent and supercritical CO₂, the membranes porosity and average pore size near the center position increased. These results reveal that the influence of different solvents on the morphology of scaffolds in the phase inversion process is significant.

Fig. 2 shows the SEM images of the cross section of the scaffolds prepared from different organic solvents and the images of local magnification. From these images, it is noticeable that the structure obtained was strongly dependent on the solvent used. When PLLA was precipitated from the dichloromethane solution, a micro pore structure was obtained; pore size ranged from 10 μm to 50 μm, and the pore wall was thick and dense. However, the scaffolds obtained from the 1,4-dioxane solution presented a nanofibrous network structure, which was not observed in the PLLA scaffolds precipitated from dichloromethane. Furthermore, the scaffolds processed from the 1,4-dioxane solution presented



Fig. 1. Optical image of PLLA scaffold prepared by supercritical phase inversion process.

a homogeneous nanofibrous structure and a cell size below 10 μm, with both micro and nanometer pores. When the mixture solution of dichloromethane/1,4-dioxane was used, the scaffolds obtained presented a homogeneous micro cell structure; the inner pore wall was rough and consisted of nanoscale cells. It was also observed that the size of the large pores formed by the porogen was identical to that of the AB particles.

The formation mechanism of the porous scaffold in this study can be proposed as follows. After the polymer/salt/solvent compound was placed in the supercritical CO₂, some amounts of the organic solvents were extracted from the compound by the supercritical CO₂ and the concentration gradient of polymer was formed. Then, the supercritical CO₂ was diffused into the sample, thus inducing a phase separation and generating a polymer-rich phase and a polymer-lean phase. When the supercritical CO₂ came out of the scaffold, the organic solvents in the scaffold were extracted by the supercritical CO₂. After the flushing of scaffold by CO₂, the dried nanofibrous structure was obtained. The process involves a ternary mixture (solvent, nonsolvent and polymer) interaction [30], the porous structure was influenced by the interaction between liquid–liquid phase and liquid–solid phase [31]. Such as, when the phase inversion takes place at a dichloromethane solution, the lower viscosity of the solution results in a slower phase inversion rate, which providing a longer phase inversion time to form larger pores. At the same time, the cellular structures may be influenced by the addition of porogen. On the one hand, the addition of porogen could in favor of the heterogeneous nucleation of the polymer-lean phase, which would form the structure with smaller pores [32]; On the other hand, the increase in viscosity by the addition of porogen may decrease the crystallization rate and provide a longer phase inversion time to form larger pores [33].

The formation of micro pores on the scaffolds prepared from the dichloromethane solution is related to the low boiling point (40 °C)

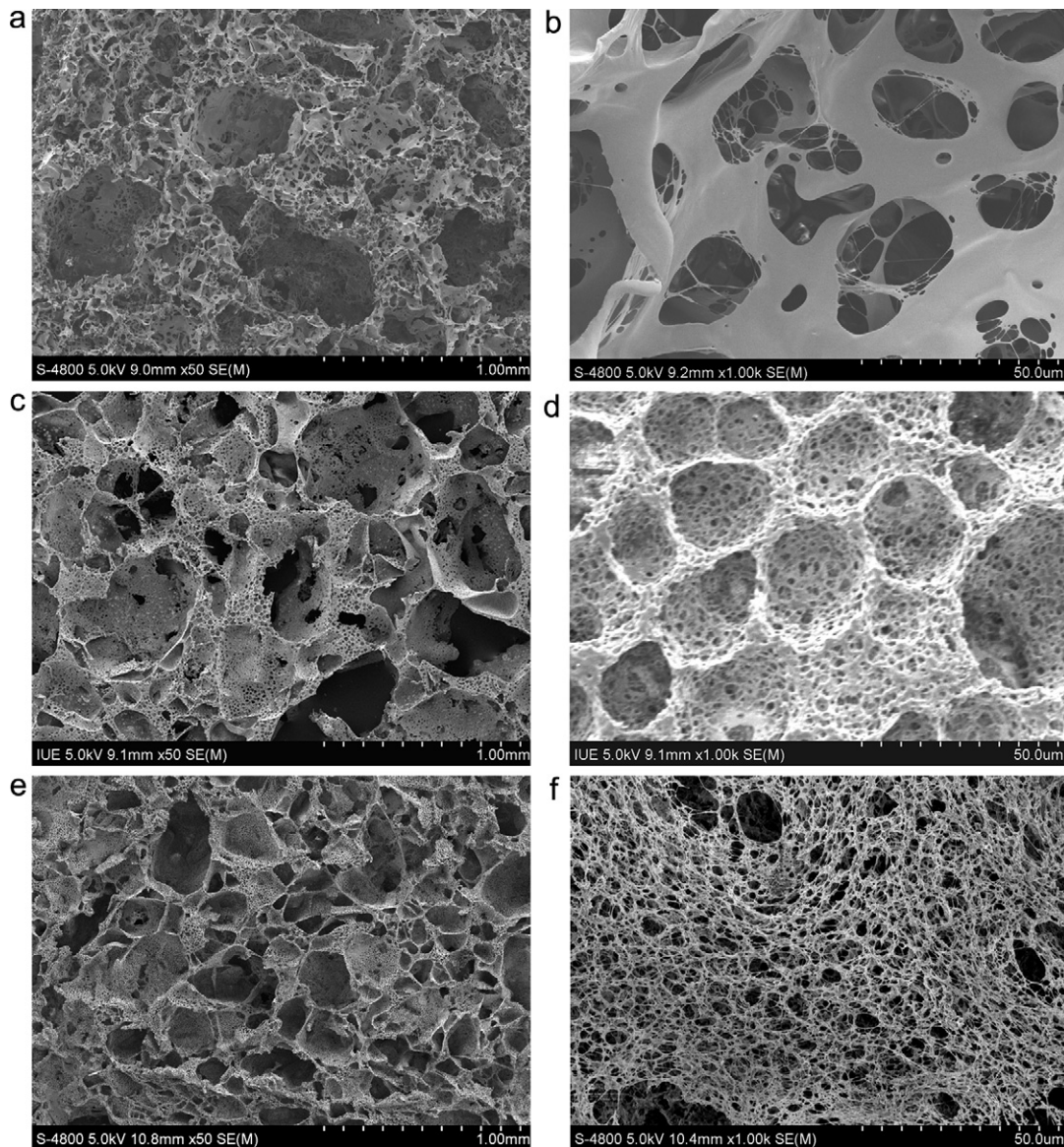


Fig. 2. SEM images of the scaffolds prepared from different organic solutions at 35 °C and 15.0 MPa: dichloromethane (a) 50 \times , (b) 1000 \times , dichloromethane/1,4-dioxane (1:1) (c) 50 \times , (d) 1000 \times ; 1,4-dioxane (e) 50 \times , (f) 1000 \times .

of the organic solvent, as this is close to the operating temperature (35 °C). The solubility of dichloromethane in the supercritical CO₂ is higher than that of 1,4-dioxane, which will favor the phase inversion process because a higher affinity of the solvent to the supercritical CO₂ will cause phase inversion and precipitation of the polymer with a porous structure. Conversely, 1,4-dioxane solution is an organic solvent with a relatively high boiling point of 101 °C, which is above the operating temperature. A lower solvent affinity, that is, a higher square solubility parameter difference, will result in a decrease in the pore size of the scaffold, and this is favorable for the formation of nanofibers. At the same time, the viscosity of the solution will influence the average pore size. Since the viscosity of dichloromethane is lower than that of 1,4-dioxane, the coarsening of the micro droplets of the polymer-lean phase, which may lead to larger pores, is favored [34,35]. These results demonstrate that completely different morphologies can be obtained from precipitation with different solvents.

It has been proved that cell behavior can be mainly determined by the substrate that they are cultured on, and the understanding of interaction mechanism between cell and nano-topography

structures could provide valuable information for the design of tissue engineering [36]. The nanofibrous structure may influence the cell differentiation, migration and protein absorption [37,38]. Three kinds of nano-topography structures have been prepared by the supercritical phase inversion technology in this experiment, it may very meaningful to induce cell growth on the scaffolds produced, to verify the effect of the mechano-topographic modulation structure of the scaffold on the preferential differentiation of the cells on next step.

3.2. Porosity and mechanical strength of scaffold

In general, an increase in porosity will decrease the compressive strength of the scaffold, and vice versa. Hence, it is important to deal with such relations well as porosity-porogen/PLLA ratio and compressive strength – porogen/PLLA ratio. In this study, different ratios of AB to PLLA were tested to find a suitable ratio to achieve a high porosity and acceptable mechanical strength. Fig. 3 shows the influence of the different ratios of AB to PLLA on the porosity and mechanical strength of the scaffold. When the mass ratio of

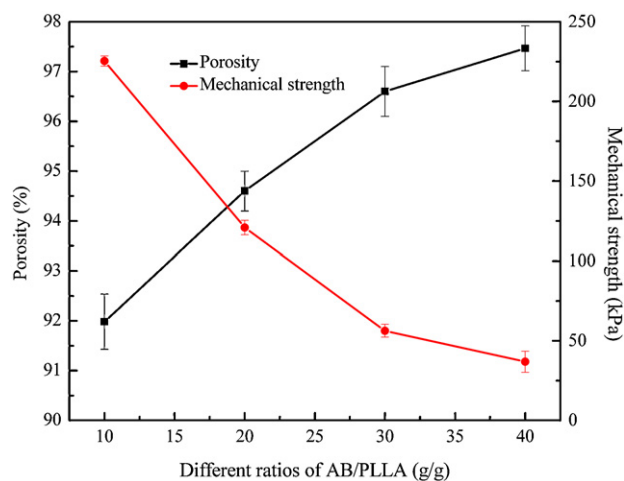


Fig. 3. The influence of the different ratios of AB to PLLA on porosity and mechanical strength (at 25% strain).

AB to PLLA increased from 10 to 40, the porosity of the scaffold was significantly increased ($P < 0.05$), from $92.0\% \pm 0.55$ to $97.5\% \pm 0.45$; however, the mechanical strength was significantly decreased from $225.4 \text{ kPa} \pm 3.16$ to $36.8 \pm 6.6 \text{ kPa}$ ($P < 0.05$). The requirement of mechanical resistance and porosity depends on the organs to be regenerated; for instance, 100 kPa is necessary for bone scaffolds [39]. At the same time, the SEM image (Fig. 4) shows that the average pore size increased with the increase in AB/PLLA ratio. These results reveal that scaffolds with desirable properties for different organs could be obtained by adjusting the ratios of AB to PLLA.

3.3. Solvent residue and analysis

Without further treatment, the dichloromethane residue in the scaffold was only 12 ppm; this is much lower than the limit of

the USP 467 Pharmacopeia (600 ppm). Although organic solvents were employed, the use of supercritical CO_2 allowed their complete removal; as the supercritical CO_2 has good diffusivity and mass transfer properties, its ability to diffuse and penetrate into the bulk of the 3D matrix allowed the complete extraction of the organic solvents [21]. Reverchon and Ji [28,40] also reported that supercritical CO_2 technology could produce a scaffold with an organic residue of less than 5 ppm and 10 ppm, respectively. However, the residual dichloromethane content of the scaffolds fabricated using the electrospinning method was 365 ppm after freeze drying for seven days [41], which is much higher than that of scaffolds prepared by supercritical CO_2 technology without further downstream processing. These results indicate that supercritical CO_2 technology is an effective method of producing a scaffold with little or no organic residue.

3.4. FTIR analysis

The FTIR spectra of the as-received PLLA and PLLA scaffolds are shown in Fig. 5. In these spectra, the PLLA characteristic bands are present; for example, the band at 1762 cm^{-1} was attributed to C=O stretching, the bands at 2949 and 2997 cm^{-1} were assigned to the CH_3 and CH stretch bands, the 1196 cm^{-1} band was assigned to the stretching of C–O–C, and the 1093 cm^{-1} band was assigned to C–O stretching. After supercritical CO_2 processing, there was no change in the chemical composition of the samples; the results were consistent with the report by Kang [42]. These results indicate that the supercritical- CO_2 -assisted phase inversion process is a physical process capable of producing PLLA scaffolds.

3.5. XRD and DSC analysis

To investigate the physical state of PLLA before and after the supercritical CO_2 processing, XRD analysis was performed. Fig. 6 shows the XRD spectra of the as-received PLLA and the PLLA scaffold. The main peaks at 16.3° and 18.5° proved the presence of

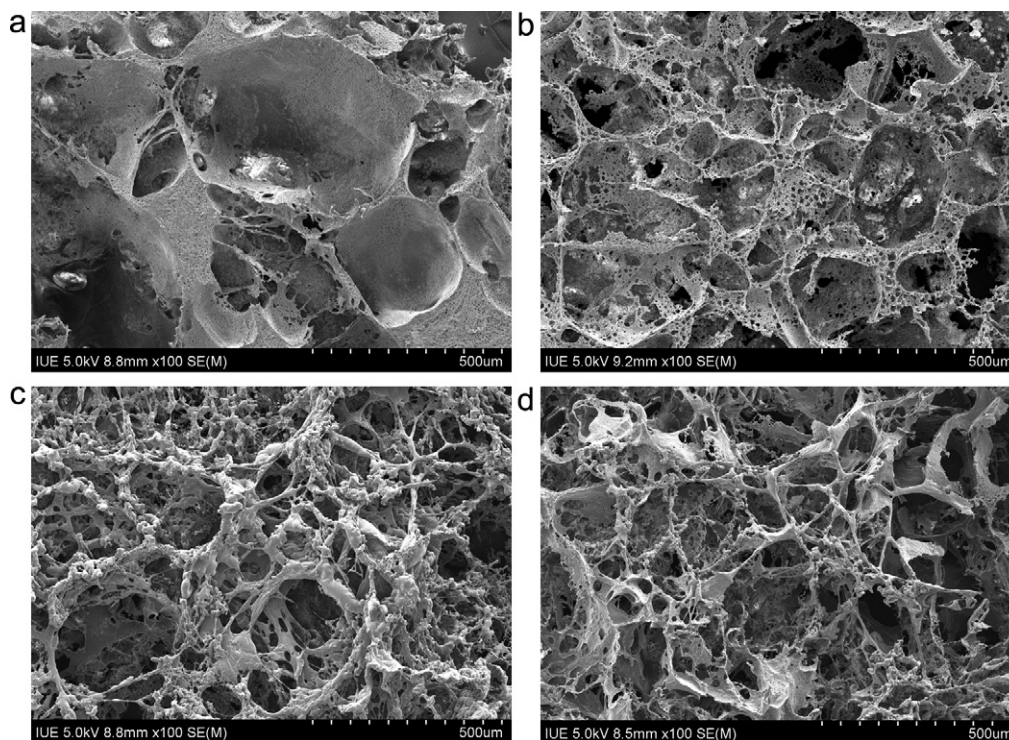


Fig. 4. SEM images of the scaffolds prepared from different AB/PLLA ratios: (a) 10:1, (b) 20:1, (c) 30:1, (d) 40:1.

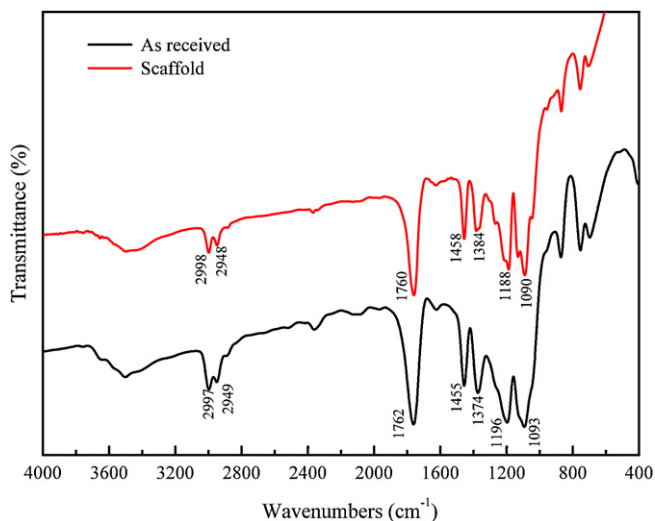


Fig. 5. FTIR spectra of as-received PLLA and the scaffold prepared by the supercritical fluid process.

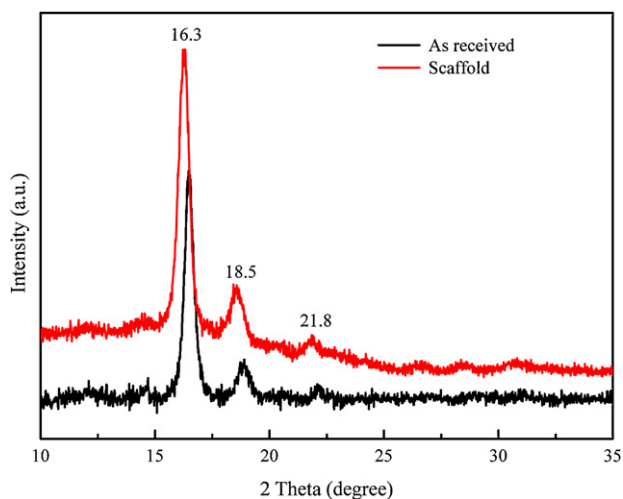


Fig. 6. XRD spectra of as-received PLLA and the scaffold prepared by the supercritical fluid process.

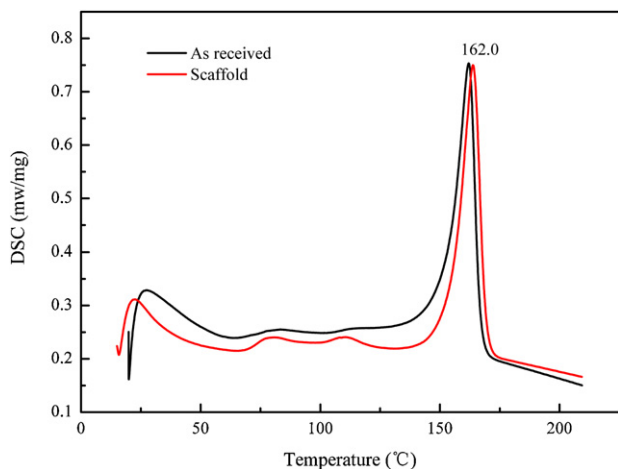


Fig. 7. DSC curves of as-received PLLA and the scaffold prepared by the supercritical fluid process.

semi-crystalline domains of PLLA specimens. Despite treating by the supercritical CO₂ process, XRD analysis showed that PLLA sample was still in semi-crystalline state. This result was similar to the previous study [43]. The DSC curves in Fig. 7 show that PLLA was observed as a semi-crystalline polymer with a melting temperature (T_m) of about 162.0 °C. The melting temperatures of the as-received PLLA and the scaffold are slightly shifted to a higher temperature, indicating that the supercritical-CO₂-assisted phase inversion process may not affect the crystallization of PLLA significantly [43,44].

4. Conclusion

Nanofibrous PLLA scaffolds with interconnected pores were successfully prepared using ammonium bicarbonate as a pore forming agent in a supercritical CO₂ process. The scaffolds possess the structural characteristics of large pores and micro and nanometer pores that have to be simultaneously present for tissue engineering applications. They are characterized by a high porosity (up to 97.5%), a fibrous structure that allows cell growth, a controllable cell size (depending on the particle size of AB), adequate mechanical properties, and almost no solvent residues. Moreover, it is possible to solve the problem of loss of the growth factors in the scaffold that occurs during the traditional preparation methods.

Acknowledgements

Financial support from the National Natural Science Foundation of China (31170939, 81171471 and 51103049) and National Science Foundation of Fujian Province (2010J05027 and 2011501223) gratefully acknowledged.

References

- [1] J.P. Chen, C.H. Su, Surface modification of electrospun PLLA nanofibers by plasma treatment and cationized gelatin immobilization for cartilage tissue engineering, *Acta Biomaterialia* 7 (2011) 234–243.
- [2] M.R. Jung, I.K. Shim, E.S. Kim, Y.J. Park, Y.I. Yang, S.K. Lee, S.J. Lee, Controlled release of cell-permeable gene complex from poly(L-lactide) scaffold for enhanced stem cell tissue engineering, *Journal of Controlled Release* 152 (2011) 294–302.
- [3] Q.W. Zhang, V.N. Mochalin, I. Neitzel, K. Hazeli, J.J. Niu, A. Kotsos, J.G. Zhou, P.I. Lelkes, Y. Gogotsi, Mechanical properties and biomineralization of multifunctional nanodiamond-PLLA composites for bone tissue engineering, *Biomaterials* 33 (2012) 5067–5075.
- [4] A.Z. Chen, X.M. Pu, Y.Q. Kang, L. Liao, Y.D. Yao, G.F. Yin, Preparation of 5-Fluorouracil-poly(L-lactide) microparticles using solution-enhanced dispersion by supercritical CO₂, *Macromolecular Rapid Communications* 27 (2006) 1254–1259.
- [5] J.M. Corey, C.C. Gertz, B.S. Wang, L.K. Birrell, S.L. Johnson, D.C. Martin, E.L. Feldman, The design of electrospun PLLA nanofiber scaffolds compatible with serum-free growth of primary motor and sensory neurons, *Acta Biomaterialia* 4 (2008) 863–875.
- [6] H.C. Liu, I.C. Lee, J.H. Wang, S.H. Yang, T.H. Young, Preparation of PLLA membranes with different morphologies of culture of MG-63 cells, *Biomaterials* 25 (2004) 4047–4056.
- [7] Z.W. Ma, C.Y. Gao, Y.H. Gong, J.C. Shen, Cartilage tissue engineering PLLA scaffold with surface immobilized collagen and basic fibroblast growth factor, *Biomaterials* 26 (2005) 1253–1259.
- [8] Z.P. Zhang, J. Hu, P.X. Ma, Nanofiber-based delivery of bioactive agents and stem cells to bone sites, *Advanced Drug Delivery Reviews* 64 (2012) 1129–1141.
- [9] G.B. Wei, P.X. Ma, Partially nanofibrous architecture of 3D tissue engineering scaffolds, *Biomaterials* 30 (2009) 6426–6434.
- [10] J.F. Mao, S. Duan, A. Song, Q. Cai, X.L. Deng, X.P. Yang, Macroporous and nanofibrous poly(lactide-co-glycolide)(50/50) scaffolds via phase separation combined with particle-leaching, *Materials Science and Engineering C* 32 (2012) 1407–1414.
- [11] A. Salerno, E.D. Maio, S. Iannace, P.A. Netti, Tailoring the pore structure of PCL scaffolds for tissue engineering prepared via gas foaming of multi-phase blends, *Journal of Porous Materials* 19 (2012) 181–188.
- [12] S. Rajabzadeh, C. Liang, Y. Ohmukai, T. Maruyama, H. Matsuyama, Effect of additives on the morphology and properties of poly(vinylidene fluoride) blend hollow fiber membrane prepared by the thermally induced phase separation method, *Journal of Membrane Science* 423–424 (2012) 189–194.
- [13] A.R.C. Duarte, J.F. Mano, R.L. Reis, Novel 3D scaffolds of chitosan-PLLA blends for tissue engineering applications: Preparation and characterization, *Journal of Supercritical Fluids* 54 (2010) 282–289.

- [14] E. Reverchon, S. Cardea, Supercritical fluids in 3-D tissue engineering, *Journal of Supercritical Fluids* 69 (2012) 97–107.
- [15] A.R.C. Duarte, J.F. Mano, R.L. Reis, Perspectives on: Supercritical fluid technology for 3D tissue engineering scaffold applications, *Journal of Bioactive and Compatible Polymers* 24 (2009) 385–400.
- [16] Y.R. Xin, T. Fujimoto, H. Uyama, Facile fabrication of polycarbonate monolith by non-solvent induced phase separation method, *Polymer* 53 (2012) 2847–2853.
- [17] F.J. Hua, T.G. Park, D.S. Lee, A facile preparation of highly interconnected macroporous poly(D,L-lactic acid-co-glycolic acid)(PLGA) scaffolds by liquid–liquid phase separation of a PLGA-dioxane-water ternary system, *Polymer* 44 (2003) 1911–1920.
- [18] E. Danesh, S.R. Ghaffarian, P. Molla-Abbasi, Non-solvent induced phase separation as a method for making high-performance chemiresistors based on conductive polymer nanocomposites, *Sensors and Actuators B* 155 (2011) 562–567.
- [19] A.R.C. Duarte, J.F. Mano, R.L. Reis, The role of organic solvent on the preparation of chitosan scaffolds by supercritical assisted phase inversion, *Journal of Supercritical Fluids* 72 (2012) 326–332.
- [20] H. Matsuyama, A. Yamamoto, H. Yano, T. Maki, M. Teramoto, K. Mishima, K. Matsuyama, Effect of organic solvents on membrane formation by phase separation with supercritical CO₂, *Journal of Membrane Science* 204 (2002) 81–87.
- [21] E. Reverchon, R. Adami, S. Cardea, G.D. Porta, Supercritical fluids processing of polymers for pharmaceutical and medical applications, *Journal of Supercritical Fluids* 47 (2009) 484–492.
- [22] D.J. Mooney, D.F. Baldwin, N.P. Suh, J.P. Vacanti, R. Langer, Novel approach to fabricate porous sponges of poly(D,L-lactic-co-glycolic acid) without the use of organic solvents, *Biomaterials* 17 (1996) 1417–1422.
- [23] I. Tsvintzelis, E. Pavlidou, C. Panayiotou, Porous scaffolds prepared by phase inversion using supercritical CO₂ as antisolvent I. Poly(L-lactic acid), *Journal of Supercritical Fluids* 40 (2007) 317–322.
- [24] L.D. Harris, B.S. Kim, D.J. Mooney, Open pore biodegradable matrices formed with gas foaming, *Journal of Biomedical Materials Research* 42 (1998) 396–402.
- [25] O.R. Davies, A.L. Lewis, M.J. Whitaker, H.Y. Tai, K.M. Shakesheff, S.M. Howdle, Applications of supercritical CO₂ in the fabrication of polymer systems for drug delivery and tissue engineering, *Advanced Drug Delivery Reviews* 60 (2008) 373–387.
- [26] G.B. Wei, P.X. Ma, Macroporous and nanofibrous polymer scaffolds and polymer/bone-like apatite composite scaffolds generated by sugar spheres, *Journal of Biomedical Materials Research* 78 (2006) 306–315.
- [27] P.X. Ma, R.Y. Zhang, Synthetic nano-scale fibrous extracellular matrix, *Journal of Biomedical Materials Research* 46 (1999) 60–72.
- [28] E. Reverchon, S. Cardea, C. Rapuano, A new supercritical fluid-based process to produce scaffolds for tissue replacement, *Journal of Supercritical Fluids* 45 (2008) 365–373.
- [29] Y.S. Nam, J.J. Yoon, T.G. Park, A novel fabrication method of macroporous biodegradable polymer scaffolds using gas foaming salt as a porogen additive, *Journal of Biomedical Materials Research* 53 (2000) 1–7.
- [30] M. Temtem, L.M.C. Silva, P.Z. Andrade, F. dos Santos, C.L. da Silva, J.M.S. Cabral, M.M. Abecasis, A. Aguiar-Ricardo, Supercritical CO₂ generating chitosan devices with controlled morphology. Potential application for drug delivery and mesenchymal stem cell culture, *Journal of Supercritical Fluids* 48 (2009) 269–277.
- [31] Y.W. Kho, D.S. Kalika, B.L. Knutson, Precipitation of nylon 6 membranes using compressed carbon dioxide, *Polymer* 42 (2006) 6119–6127.
- [32] I. Tsvintzelis, S.J. Marras, I. Zubrtikudis, C. Panayiotou, Porous poly(L-lactic acid) nanocomposite scaffolds prepared by phase inversion using supercritical CO₂ as antisolvent, *Polymer* 48 (2007) 6311–6318.
- [33] J.H. Lee, T.G. Park, H.S. Park, D.S. Lee, Y.K. Lee, S.C. Yoon, J.D. Nam, Thermal and mechanical characteristics of polymer(L-lactic acid) nanocomposite scaffold, *Biomaterials* 24 (2003) 2773–2778.
- [34] H. Matsuyama, H. Yano, T. Maki, M. Teramoto, K. Mishima, K. Matsuyama, Formation of porous flat membrane by phase separation with supercritical CO₂, *Journal of Membrane Science* 194 (2001) 157–163.
- [35] E. Reverchon, S. Cardea, Formation of cellulose acetate membranes using a supercritical fluid assisted process, *Journal of Membrane Science* 240 (2004) 187–195.
- [36] V. Beachley, X.J. Wen, Polymer nanofibrous structures: Fabrication, biofunctionalization, and cell interactions, *Progress in Polymer Science* 35 (2010) 868–892.
- [37] S.H. Lim, X.Y. Liu, H.J. Song, K.J. Yarema, H.Q. Mao, The effect of nanofiber-guided cell alignment on the preferential differentiation of neural stem cells, *Biomaterials* 31 (2010) 9031–9039.
- [38] A.S. Nathan, B.M. Baker, N.L. Nerurkar, R.L. Mauck, Mechano-topographic modulation of stem cell nuclear shape on nanofibrous scaffolds, *Acta Biomaterialia* 7 (2011) 57–66.
- [39] J.C. Zhang, H. Zhang, L.B. Wu, J.D. Ding, Fabrication of three dimensional polymeric scaffolds with spherical pores, *Journal of Materials Science* 41 (2006) 1725–1731.
- [40] C.D. Ji, N. Annabi, M. Hosseinkhani, S. Sivaloganathan, F. Dehghani, Fabrication of poly-DL-lactide/polyethylene glycol scaffolds using the gas foaming technique, *Acta Biomaterialia* 8 (2012) 570–578.
- [41] H.M. Nie, C.H. Wang, Fabrication and characterization of PLGA/Hap composite scaffolds for delivery of BMP-2 plasmid DNA, *Journal of Controlled Release* 120 (2007) 111–121.
- [42] Y.Q. Kang, C. Yang, P. Ouyang, G.F. Yin, Z.B. Huang, Y.D. Yao, X.M. Liao, The preparation of BSA-PLLA microparticles in a batch supercritical anti-solvent process, *Carbohydrate Polymers* 77 (2009) 244–249.
- [43] A. Vega-Gonzalez, P. Subra-Paternault, A.M. Lopez-Periago, C.A. Garcia-Gonzalez, C. Domingo, Supercritical CO₂ antisolvent precipitation of polymer networks of L-PLA, PMMA and PMMA/PCL blends for biomedical applications, *European Polymer Journal* 44 (2008) 1081–1094.
- [44] S.Y. Huang, H.F. Li, S.C. Jiang, X.S. Chen, L.J. An, Crystal structure and morphology influenced by shear effect of poly(L-lactide) and its melting behavior revealed by WAXD, DSC and in situ POM, *Polymer* 52 (2011) 3478–3487.